An EPR and ^{1}H NMR Active Mixed-Valence Manganese (III/II/III) Trinuclear Compound

Vasilis Tangoulis,[†] Dora A. Malamatari,[‡] Georgios A. Spyroulias,[§] Catherine P. Raptopoulou,[†] Aris Terzis,[†] and Dimitris P. Kessissoglou*[,‡]

Department of General & Inorganic Chemistry, Aristotle University of Thessaloniki, 54006 Thessaloniki, Greece, NRCPS "Demokritos", Institute of Materials Science, 15310 Aghia Paraskevi Attikis, Greece, and Department of Chemistry, University of Florence, Florence, Italy

Received December 15, 1999

A mixed-valence Mn(III)−Mn(II)−Mn(III) trinuclear complex of stoichiometry $Mn^{III}Mn^{II}Mn^{III}(Hsaladhp)_2(Sal)_4\cdot 2CH_3CN$ (**1**), where H_3saladhp is a tridentate Schiff-base ligand, has been structurally characterized with X-ray crystallography. The Mn(III)Mn(II)Mn(III) angles are strictly 180° as required by crystallographic inversion symmetry. The complex is valence-trapped with two terminal Mn(III) ions in a distorted square pyramidal geometry. The Mn(III)···Mn(II) separation is 3.495 Å. The trinuclear complex shows small antiferromagnetic exchange J coupling. The magnetic parameters obtained from the fitting procedure in the temperature range 10−300 K are $J_1 = -5.7$ cm^{-1}, $g = 2.02$, $zJ = -0.19$ cm^{-1}, and $R = 0.004$. The EPR spectrum was obtained at 4 K in $CHCl_3$ and in tetrahydrofuran glasses. The low-field EPR signal is a superposition of two signals, one centered around $g = 3.6$ and the other, for which hyperfine structure is observed, centered around $g = 4.1$ indicating an $S = {}^3/_2$ state. In addition, there is a 19-line signal at $g = 2.0$. The multiline signal compares well with that observed for the S_2 or S_0* states of the oxygen-evolving complex. ^{1}H NMR data reveal that the trinuclear compound keeps its integrity into the $CHCl_3$ solution. Crystal data for complex **1**: $[C_{54}H_{52}N_4O_{18}Mn_3]$, $M = 1209.82$, triclinic, space group $P\bar{1}$, $a = 10.367(6)$ Å, $b = 11.369(6)$ Å, $c = 13.967(8)$ Å; $\alpha = 112.56(1)°$, $\beta = 93.42(2)°$, $\gamma = 115.43(1)°$, $Z = 1$.

Introduction

One of the most important processes in Nature occurs in the oxygen-evolving complex (OEC) of photosystem II (PSII), where the four-electron oxidation of water to molecular oxygen is believed to be catalyzed by a cluster of four manganese ions.[1] The available data strongly suggest that a polynuclear cluster is responsible for the observed EPR signals of the "active form" of S_1 ($g = 4.8$ in parallel polarization) and S_2 ($g = 2$ multiline and $g = 4.1$ with fine structure) oxidation states of the OEC.[2−5] In addition, extended X-ray absorption fine structure (EXAFS) data[6] indicate the presence of at least two ∼2.7 Å Mn···Mn interactions in addition to an ∼3.3 Å interaction. The manganese coordination sphere is believed to be dominated by O and N donors from available amino acid side chains.[7] Dismukes and Siderer[2] published the first observation of an EPR signal attributable to a multinuclear Mn center in PSII. In X-band EPR spectra the $g = 2$ multiline EPR signal from PSII typically exhibits 19 or more partially resolved hyperfine lines.[2] Model compounds such as those with mixed-valence,[8−10] di-μ-oxo-

[†] Institute of Materials Science.
[‡] Aristotle University of Thessaloniki.
[§] University of Florence.

(1) (a) Pecoraro, V. L. *Manganese Redox Enzymes;* VCH Publishers Inc.; New York, 1992; (b) Dismukes, G. C. *Photochem. Photobiol.* **1986**, *43*, 99. (c) Yachandra, V. K.; Sauer, K.; Klein, M. P. *Chem. Rev.* **1996**, *96*, 2927.
(2) Dismukes, G. C.; Siderer, Y. *Proc. Natl. Acad. Sci. USA* **1981**, *78*, 274.
(3) (a) Cooper, S. R.; Dismukes, G. C.; Klein, M. P.; Calvin, M. *J. Am. Chem. Soc.* **1978**, *100*, 7248; (b) Kawasaki, H.; Kusunoki, M.; Hayashi, Y.; Suzuki, M.; Munezawa, K.; Suenaga, M.; Senda, H.; Uehara, A. *Bull. Chem. Soc. Jpn.* **1994**, *67*, 1310; (c) Manhanda, R.; Brudvig, G. W.; de Gala, S.; Crabtree, R. H. *Inorg. Chem.* **1994**, *33*, 5157; (d) Philouze, C.; Blondin, G.; Girerd, J.-J.; Guilhem, J.; Rascard, C.; Lexa, D. *J. Am. Chem. Soc.* **1994**, *116*, 8557.
(4) (a) Casey, J.; Sauer, K. *Biochim. Biophys. Acta* **1984**, *767*, 21. (b) Zimmermann, J.-L.; Rutherford, A. W. *Biochemistry* **1986**, *25*, 4609. (c) Rutherford, A. W.; Boussac, A.; Zimmermann, J. L. *New J. Chem.* **1991**, *15*, 491.
(5) (a) dePaula, J. C.; Beck, W. F.; Brudving, G. W. *J. Am. Chem. Soc.* **1986**, *108*, 4002. (b) Hansson,O. R.; Aasa, R.; Vanngard, T. *Biophys. J.* **1987**, *51*, 825. (c) Kim, D. H.; Britt, R. D.; Klein, M. P.; Sauer, K. *Biochemistry* **1992**, *31*, 541. (d) Dexheimer, S. L.; Klein, M. P. *J. Am. Chem. Soc.* **1992**, *114*, 2821. (e) Randall, D. W.; Sturgeon, B. E.; Ball, J. A.; Lorigan, G. A.; Chan, M. K.; Klein, M. P.; Armstrong, W. H.; Britt, R. D. *J. Am. Chem. Soc.* **1995**, *117*, 11780. (f) Miller, A−F.; Brudving, G. W. *Biochim. Biophys. Acta* **1984**, *767*, 160.
(6) (a) Guiles, R. D.; Yachandra, V. K.; McDermott, A. E.; Cole, J. L.; Dexheimer, S. L.; Britt, R. D.; Sauer, K.; Klein, M. P. *Biochemistry* **1990**, *29*, 486. (b) George, G. N.; Prince, R. C.; Cramer, S. P. *Science* **1989**, *243*, 789. (c) Penner-Hahn, J. E.; Fronko, R. M.; Pecoraro, V. L.; Yocum, C. F.; Betts, S. D.; Bowlby, N. R. *J. Am. Chem. Soc.* **1990**, *112*, 2549. (d) Riggs-Gelasco, P. J.; Mei, R.; Yocum, C. F.; Penner-Hahn, J. E. *J. Am. Chem. Soc.* **1996**, *118*, 2387. (e) Yachandra, V. K.; DeRose, V. J.; Latimer, M. J.; Mukerji, I.; Sauer, K.; Klein, M. P. *Science* **1993**, *260*, 675. (f) DeRose, V. J.; Mukerji, I.; Latimer, M. J.; Yachandra, V. K.; Sauer, K.; Klein, M. P. *J. Am. Chem. Soc.* **1994**, *116*, 5239. (g) Riggs-Gelasco, P. J.; Mei, R.; Ghanotakis, D.; Yocum, C. F.; Penner-Hahn, J. E. *J. Am. Chem. Soc.* **1996**, *118*, 2400. (j) Dau, H.; Andrews, J. C.; Roelofs, T. A.; Latimer, M. J.; Liang, W.; Yachandra, V. K.; Sauer, K.; Klein, M. P. *Biochemistry* **1995**, *34*, 5274.
(7) (a) Tamura, N.; Ikeuchi, M.; Inoue, Y. *Biochim. Biophys. Acta* **1989**, *973*, 281. (b) Andreasson, L.-e. *Biochim. Biophys. Acta* **1989**, *973*, 465.
(8) Eppley, H. J.; Tsai, H.-L.; de Vries, N.; Folting, K.; Christou, G.; Hendrickson, D. N. *J. Am. Chem. Soc.* **1995**, *117*, 301. (b) Tsai, H.-L.; Wang, S.; Folting, K.; Streib, W. E.; Hendrickson, D. N.; Christou, G. *J. Am. Chem. Soc.* **1995**, *117*, 2503. (c) McCusker, J. K.; Jang, H. G.; Wang, S.; Christou, G.; Hendrickson, D. N. *Inorg. Chem.* **1992**, *31*, 1874. (d) Wieghardt, K. *Angew. Chem., Int. Ed. Engl.* **1994**, *33*, 725. (e) Wieghardt, K. *Angew. Chem., Int. Ed. Engl.* **1989**, *28*, 1153. (f) Auger, N.; Girerd, J.-J.; Corbella, M.; Gleizes, A.; Zimmerman, J.-L. *J. Am. Chem. Soc.* **1990**, *112*, 448.
(9) Vincent, J. B.; Christou, G. *Adv. Inorg. Chem. Radiochem.* 1989, *33*, 197.

10.1021/ic991430x CCC: $19.00
Published on Web 05/20/2000

bridged $Mn^{III}Mn^{IV}$ ions give rise to $g = 2$ EPR signals with 16 well-resolved lines with a regular spacing of about 80 G. The differences between these signals and those of the binuclear model complexes could be caused by the PSII signal originating from a cluster with more than two Mn ions. Casey and Sauer[4a] and Zimmermann and Rutherford[4b] determined that the $g = 4.1$ signal of OEC arises from the S_2 state. Although it is believed that the knowledge gained from EPR studies[2−5] supports the presence of a single cluster of four magnetically coupled Mn atoms, the structural motif of trimer−monomer, (3Mn + 1Mn),[1a] makes it necessary to investigate trinuclear mixed-valence manganese complexes as well.

Previous efforts have centered on the preparation and characterization of trinuclear complexes with predominantly oxygen-donor ligands to understand the fundamental coordination, structure, and magnetochemistry of complexes potentially relevant to the active site of the OEC.[11−20] In this report, we present an EPR study of a mixed-valence Mn(II)−Mn(III) trinuclear compound showing characteristics very similar to those of the EPR signal of the S_2 or S_0* states of PSII. For the first time a ^{1}H NMR study of mixed-valence manganese-trimer compounds is also reported. ^{1}H NMR data reveal that the trinuclear compound keeps its integrity in the $CHCl_3$ solution. The crystal structure of $Mn^{III}Mn^{II}Mn^{III}(Hsaladhp)_2(Sal)_4 \cdot 2CH_3CN$ is also the first example of an open mixed-valence Mn(II)−Mn(III) trinuclear compound with five coordinated terminal atoms.

Experimental Section

The following abbreviations are used throughout the text: H_3saladhp, 1,3-dihydroxy-2-methyl(salicylideneamino)propane; HOAc, acetic acid; H_2sal, salicylic acid; H_2hib, 2-hydroxyisobutyric acid; dmf, dimethylformamide; thf, tetrahydrofuran.

Materials. The chemicals for the synthesis of the compounds were used as purchased. Acetonitrile (CH_3CN) was distilled from calcium hydride (CaH_2) and CH_3OH from magnesium (Mg) and were stored over 3 Å molecular sieves. Diethyl ether, anhydrous grade, and absolute ethanol were used without any further purification. Salicylaldehyde, 5-chlorosalicylaldehyde, 2-amino-2-methyl-1,3-propandiol, salicylic acid, 5-chlorosalicylic acid, and $Mn(AcO)_2 \cdot 4H_2O$ were purchased from Aldrich Co. All chemicals and solvents were reagent grade.

Physical Measurements. The NMR spectra of the mixed-valence manganese(III/II/III) trinuclear compound were acquired using MSL 200 and DRX 500 Bruker spectrometers operating at 200.13 and 500.13 MHz Larmor frequencies, respectively. The spectra were calibrated by assigning the residual chloroform signal a shift from tetramethylsilane (TMS) of 7.24 ppm at 296 K. Longitudinal relaxation rates were measured at 500 MHz, using a nonselective inversion recovery pulse sequence.[21] The T_1 values were obtained from a three-parameter fit of the data to an exponential recovery function. In every case the magnetization recovery is exponential within the accuracy of the experiment, as expected for fast-relaxing nuclei with little cross-relaxation.[22,23] One-dimensional nuclear Overhauser effect (1D NOE) spectra were recorded in a difference mode using acquisition schemes described elsewhere.[24,25] The standard Bruker software package was used for data processing.[26−28] Infrared spectra (400−4000 cm^{-1}) were recorded on a Perkin-Elmer FT-IR 1650 spectrometer with samples prepared as KBr pellets. UV−vis spectra were recorded on a Shimadzu-160A dual beam spectrophotometer. Electron spin resonance (ESR) spectra were recorded on a Bruker ESR 300 spectrometer equipped with a Varian variable temperature controller. 2,2-Diphenyl-1-picrylhydrazyl (DPPH) was used as an external standard. C, H, and N elemental analyses were performed on a Perkin-Elmer 240B elemental analyzer, and Mn was determined by atomic absorption spectroscopy on a Perkin-Elmer 1100B spectrophotometer. The magnetic measurements were performed on a polycrystalline sample (30.0 mg) using a Quantum Design Squid susceptometer, and 60 points were collected in the 4.00−300 K temperature range. The applied magnetic field was 1000.00 G. The correction for the diamagnetism of the complex was estimated from Pascal constants; a value of 56×10^{-6} cm^3 mol^{-1} was used for the temperature-independent paramagnetism (TIP) of the Mn ion. The magnetism of the sample was field-independent. Electric conductance measurements were performed with a WTW model LF 530 conductivity outfit and a type C cell, which had a cell constant of 0.996. This represents a mean value calibrated at 25 °C with potassium chloride. All temperatures were controlled with an accuracy of ± 0.1 °C using a Haake thermoelectric circulating system.

Preparation of the Compounds. The Schiff base was synthesized by condensation of salicylaldehyde with 2-amino-2-methyl-1,3-propanediol.

(**1**) $Mn^{III}Mn^{II}Mn^{III}(Hsaladhp)_2(Hsal)_4$. Ten millimoles (1.1 mL) of salicylaldehyde was added to a solution of 10 mmol (1.05 g) of 2-amino-2-methyl-1,3-propandiol in 100 mL of CH_3OH. The resulting mixture was refluxed for 1 h, generating a pale yellow solution. When the solution was cooled to room temperature 15 mmol of $MnCl_2 \cdot 4H_2O$ in 100 mL of methanol, 20 mmol of KNO_2 and salicylic acid in 1:1 ratio were added with stirring. This reaction mixture was refluxed for 1 h, after which the solution was allowed to cool to room temperature and was exposed to dioxygen by bubbling air into the reaction mixture. The resulting dark-brown solution after 5 h stirring was reduced in volume (10 mL), and 100 mL of acetonitrile was added. Dichroic (green/brown) crystals suitable for X-ray diffraction studies were obtained by slow evaporation. The crystalline product was characterized by elemental analysis with the formula $C_{54}H_{52}N_4O_{18}Mn_3$ (fw = 1209) $[Mn^{III}Mn^{II}Mn^{III}(Hsaladhp)_2(Hsal)_4 \cdot 2CH_3CN]$. Yield 50%. Anal. Calcd. for C, 53.59; H, 4.30; N, 4.63; Mn, 13.65. Found: C, 53.00; H, 4.50; N, 4.70; Mn, 13.10; IR(KBr pellet, cm^{-1}) ν(O−H) 3210(vs), ν(C=N):1615(vs), $\nu_{as}(CO_2)$ of horizontal salicylic acid:1590(vs), $\nu_{as}(CO_2)$ of vertical salicylic acid:1580(vs), ν(C=O):1540(s), $\nu_{sym}(CO_2)$ of horizontal salicylic acid:1425(vs), $\nu_{sym}(CO_2)$ of vertical salicylic acid: 1375(vs), UV−vis[λ (ϵ, $M^{-1} \cdot cm^{-1}$), CH_2Cl_2]: 480(1650), 380(4600), 300(14400); FAB-MS(+) (thf solution) gives molecular ion $[Mn^{III}Mn^{II}Mn^{III}(Hsaladhp)_2(Hsal)_4 \cdot 2CH_3CN]$ at m/z 1209.

(10) Christou, G. *Acc. Chem. Res.* **1989**, *22*, 328.
(11) Kessissoglou, D. P.; Butler, W. M.; Pecoraro, V. L. *J. Chem. Soc., Chem. Commun.* **1986**, 1253.
(12) Kessissoglou, D. P.; Li, X.-h.; Butler, W. M.; Pecoraro, V. L. *Inorg. Chem.* **1987**, *26*, 2487.
(13) Li, X−h.; Kessissoglou, D. P.; Kirk, M. L.; Bender, C.; Pecoraro, V. L. *Inorg. Chem.* **1988**, *27*, 1.
(14) Kessissoglou, D. P.; Kirk, M. L.; Bender, C. A.; Lah, M. S.; Pecoraro, V. L. *J. Chem. Soc., Chem. Commun.* **1989**, 84.
(15) Bonadies, J. A.; Kirk, M. L.; Lah, M. S.; Kessissoglou, D. P.; Hatfield, W. E.; Pecoraro, V. L. *Inorg. Chem.* **1989**, *28*, 2037.
(16) Kessissoglou, D. P.; Butler, W. M.; Pecoraro, V. L. *Inorg. Chem.* **1987**, *26*, 495.
(17) Kessissoglou, D. P.; Kirk, M. L.; Lah, M. S.; Li, X.-h.; Raptopoulou, C. A.; Hatfield, W. E.; Pecoraro, V. L. *Inorg. Chem.* **1992**, *31*, 5424.
(18) Malamatari, D. A.; Hitou, P.; Hatzidimitriou, A. G.; Inscore, F. E.; Gourdon, A.; Kirk, M. L.; Kessissoglou, D. P. *Inorg. Chem.* **1995**, *34*, 2493.
(19) Kirk, M. L.; Lah, M. S.; Raptopoulou, C. A.; Kessissoglou, D. P.; Hatfield, W. E.; Pecoraro, V. L. *Inorg. Chem.* **1991**, *30*, 3900.
(20) Tangoulis, V.; Malamatari, D. A.; Soulti, K.; Stergiou, V.; Raptopoulou, C. P.; Terzis, A.; Kabanos, T. A.; Kessissoglou, D. P. *Inorg. Chem.* **1996**, *35*, 4974.
(21) Vold, R. L.; Waugh, J. S.; Klein, M. P.; Phelps, D. E. *J. Chem. Phys.* **1968**, *48*, 3831−3832.
(22) La Mar, G. N.; de Ropp, J. S. *Biological Magnetic Resonance;* Berliner, L. J., Reuben, J., Eds.; Plenum Press: New York, 1993; Vol. 12, pp 1−78.
(23) Bertini, I.; Donaire, A.; Luchinat, C.; Rosato, A. Proteins *Struct. Funct. Genet.* **1997**, *29*, 348−358.
(24) Banci, L.; Bertini, I.; Luchinat, C.; Piccioli, M.; Scozzafava, A.; Turano, P. *Inorg. Chem.* **1989**, *28*, 4650−4656.
(25) Dugad, L. B.; La Mar, G. N.; Banci, L.; Bertini, I. *Biochemistry* **1990**, *29*, 2263−2271.
(26) Aue, W. P.; Bartholdi, E.; Ernst, R. R. *J. Chem. Phys.* **1976**, *64*, 2229−2235.
(27) Macura, S.; Ernst, R. R. *Mol. Phys.* **1980**, *41*, 95.
(28) Bax, A.; Davis, D. G. *J. Magn. Reson.* **1985**, *63*, 207−213.

Table 1. Summary of Crystal, Intensity Collection, and Refinement Data of **1**

formula	$C_{54}H_{52}N_4O_{18}Mn_3$
a	10.367(6) Å
b	11.369(6) Å
c	13.967(8) Å
α	112.56(1)ï
β	93.42(2)ï
γ	115.43(1)ï
V	1322.3(12) Å^3
T	298 K
space group	$P\bar{1}$
Z	1
fw	1209.82
λ	0.71073 Mo Kα
abs coeff(*μ*)	0.785 mm^{-1}
ρ_{calcd}/ρ_{obsd}	1.519/1.50 g cm^{-3}
$w^a = 1/\sigma^2(F_o^2) + (a \times P)^2 + b \times P$	$a = 0.0231$, $b = 0.6824$
R^bindices [4093 [$I > 2.0\ \sigma(I)$]	$R_1 = 0.0302$, $wR_2 = 0.0829$
	R_1 based on F values, wR_2 based on F^2

$$^a w = \frac{1}{[\sigma^2 \times (F_o^2) + (a \times P)^2 + b \times P]} \text{ and } P2 = \frac{[\max(F_o^2,0) - 2 \times F_c^2]}{3}$$

$$^b R_1 = \frac{\sum(|F_o| - |-|F_c|)}{\sum(|F_o|)}, wR_2 = \sqrt{\frac{\sum[w \times (F_o^2 - F_c^2)^2]}{\sum[w \times (F_o^2)^2]}}$$

X-ray Crystal Structure Determination. A green-brown prismatic crystal of **1** with approximate dimensions 0.20 × 0.25 × 0.50 was mounted in capillary filled with drops of mother liquid. Diffraction measurements were made on a Crystal Logic Dual Goniometer Diffractometer using graphite-monochromated Mo Kα radiation (λ = 0.710730 Å) radiation. Crystal data and parameters for data collection are reported in Table 1. Unit cell dimensions were determined and refined by using the angular settings of 25 automatically centered reflections in the range $11° < 2\theta < 23°$. The intensities of 4953 reflections were measured ($-12 \le h \le 0$, $-12 \le k \le 13$, $-16 \le l \le 16$) at room temperature $\theta-2\theta$ scan ($2.08 < 2\theta < 25.00°$) with scan speed 3.0 deg/min and scan range 2.4 plus $\alpha_1\alpha_2$ separation. Three standard reflections monitored every 97 reflections, showed <3.0% intensity fluctuation and no decay. Lorentz, polarization, and ψ-scan absorption corrections were applied using Crystal Logic software.

Symmetry equivalent data of **1** were averaged with $R(\text{int}) = 0.0106$ to give 4666 independent reflections from a total of 4953. The structure was solved by direct methods using the program SHELXS-86.[29] The refinement was performed using the program SHELXL-93.[30] Anisotropic thermal parameters were used for all non-H atoms. At the tetrahedral C(8) atom the methyl group [C(11)] and the methoxy group [C(11)−O(3)] are disordered. Therefore, O(3) has been refined in two positions [bounded to C(10) and to C(11)] with occupancy factors 0.71 [O(3)] and 0.29 [O(3A)]. The structure refined to wR2 = 0.0879 for all 4666 independent data and to R1 = 0.0302 for 4093 observed data [$(I) > 2\sigma(I)$]. The maximum and minimum residual peaks in the final difference map were 0.211 and −0.319 e/Å^3. The largest shift/estimated standard deviation (esd) in the final cycle was 0.005. Positional and *U*(equiv) thermal parameters are given in Table 2.

Results and Discussion

Synthesis. The mixed-valence trinuclear compounds of the general composition $Mn^{III}Mn^{II}Mn^{III}$(X-Hsaladhp)$_2$(Hsal)$_4$ [X = H, Cl, CH_3] can be prepared by adding the Schiff-base ligand and the salicylic acid in the presence of KNO_2 to $MnCl_2 \cdot 4H_2O$ in methanol and with exposure to air. Using $Mn(AcO)_2$ or $Mn(AcO)_3$ analogous trimers of the general composition $Mn^{III}Mn^{II}Mn^{III}$(X-Hsaladhp)$_2$(AcO)$_4$(CH_3OH)$_2$ have been isolated.[13,14,17] These trimers react with X-salicylic acid in methanol, dmf, or thf to yield mixed acetato/salicylato trinuclear complexes which are isolated as dark brown solids.[20] The reaction can take place in all three solvents leading to the formation of trinuclear compounds in contrast to the preparation of the trinuclear complexes with only acetates as bridging ligands for which, in the presence of dmf, mononuclear Mn^{IV} complexes[11,12] and MnO_2 are formed exclusively. To obtain the trinuclear compounds it is absolutely essential not to add an additional strong base, such as sodium methoxide or sodium hydroxide, that leads to mononuclear Mn^{IV} complexes. Addition of excess of salicylic acid does not lead to the total replacement of all acetates ligands by salicylates ones. We should mention that in the presence of CH_3CN the mixed acetato/salicylato bridged trinuclear complexes result to a polymeric compound with the same trimeric unit [$Mn^{III}Mn^{II}Mn^{III}$] but with significant deviation from linearity[18] ($Mn^{III} - Mn^{II} - Mn^{III} = 137.5°$). Generally nitrogen-donor solvents, e.g., CH_3CN, py, en, are not bound at the sixth position of Mn^{III} ion.

$$\text{X-}C_6H_3(OH)CHO + H_2NC(R)(CH_2OH)_2 \xrightarrow{\text{MeOH}} \text{X-}C_6H_3(O)CH{=}NC(R)(CH_2OH)_2$$

Table 2. Positional (×10^4) and Equivalent Thermal Parameters (×10^4) of the non-H Atoms[a]

atom	*x*	*y*	*z*	*U*(eq)
Mn(1)	0	0	0	30(1)
Mn(2)	3097(1)	114(1)	1260(1)	31(1)
O(1)	5101(2)	896(2)	1883(1)	40(1)
O(2)	1060(2)	−967(2)	570(1)	33(1)
N(1)	2528(2)	−970(2)	2125(1)	33(1)
O(4)	3750(2)	745(2)	176(1)	38(1)
O(5)	1987(2)	1069(2)	−488(1)	43(1)
O(7)	3144(2)	2138(2)	2195(1)	43(1)
O(8)	1000(2)	1916(2)	1525(1)	45(1)
C(1)	5769(2)	592(2)	2515(2)	35(1)
C(2)	7316(3)	1235(3)	2755(2)	44(1)
C(3)	8070(3)	992(3)	3435(2)	53(1)
C(4)	7330(3)	95(3)	3889(2)	60(1)
C(5)	5816(3)	−567(3)	3651(2)	51(1)
C(6)	5003(2)	−329(2)	2966(2)	37(1)
C(7)	3420(3)	−1038(3)	2757(2)	38(1)
C(8)	890(2)	−1721(2)	1971(2)	38(1)
C(9)	265(2)	−2165(2)	795(2)	37(1)
C(10)	513(3)	−597(3)	2728(2)	47(1)
C(11)	299(3)	−3057(3)	2184(3)	53(1)
O(3)	1302(4)	−63(4)	3798(2)	68(1)
O(3A)	515(7)	−4105(7)	1573(6)	57(2)
C(12)	3283(2)	1327(2)	−297(2)	32(1)
C(13)	4434(2)	2380(2)	−581(2)	34(1)
C(14)	4010(3)	2987(3)	−1147(2)	45(1)
C(15)	5033(3)	4011(3)	−1398(2)	54(1)
C(16)	6522(3)	4464(3)	−1068(2)	52(1)
C(17)	6968(3)	3883(3)	−509(2)	46(1)
C(18)	5943(2)	2816(2)	−280(2)	37(1)
O(6)	6493(2)	2237(2)	212(2)	54(1)
C(19)	2250(2)	2607(2)	2207(2)	34(1)
C(20)	2652(2)	4078(2)	3071(2)	34(1)
C(21)	4032(3)	4937(3)	3824(2)	47(1)
C(22)	4432(4)	6295(3)	4628(2)	60(1)
C(23)	3424(4)	6798(3)	4717(2)	58(1)
C(24)	2053(3)	5976(3)	3993(2)	53(1)
C(25)	1662(3)	4625(2)	3158(2)	40(1)
O(9)	318(2)	3893(2)	2429(2)	57(1)
N(2)	1672(4)	2797(5)	5395(4)	127(2)
C(26)	2054(4)	3938(5)	6033(4)	84(1)
C(27)	2573(7)	5388(5)	6853(6)	111(2)

[a] Estimated standard deviations stated in parentheses after the value. *U*eq = 1/3($U_{11} + U_{22} + U_{33}$).

(29) Sheldrick, G. M. *SHELX 86*; University of Goettingen: Germany, 1986.
(30) Sheldrick, G. M. *SHELX 93: Crystal Structure Refinement*; University of Goettingen: Germany, 1993.

$$X\text{-}C_6H_3(O)CH{=}NC(R)(CH_2OH)_2 + MnCl_2{\cdot}4H_2O + X\text{-}H_2Sal + KNO_2 \xrightarrow{MeOH} Mn^{III}Mn^{II}Mn^{III}[(X\text{-}C_6H_3(O)CH{=}NC(R)(CH_2O)(CH_2OH)]_2(X\text{-}Hsal)_4$$

The mixed-valence trinuclear compounds are green-black crystalline solids that appear to be stable in air. They are soluble in dimethyl sulfoxide (dmso), dmf, CH_2Cl_2, thf, and $CHCl_3$ but insoluble in water. The behavior of the complexes as electrolytes shows a different degree of dissociation in various solvents leading to the general conclusion that in CH_2Cl_2 and thf no dissociation occurs while in dmf and dmso partial dissociation is observed.

Description of Structure 1. ORTEP diagram of complex **1** is shown at Figure 1. Bond distances and angles for the coordination spheres are listed in Table 3. The complex includes a central octahedral Mn(II) ion, Mn(1), located at a crystallographic inversion center. It is flanked by two distorted square-pyramidal Mn(III) ions Mn(2). The octahedral coordination environment of the central Mn(II) ion is composed of four *syn*-bridging salicylates and two μ-alkoxo oxygen atoms of the Schiff-base ligands. The geometry at each Mn(III) center is best described as a distorted tetragonal pyramid. Using the trigonality index $\tau = (\varphi_1 - \varphi_2)/60$ where φ_1 and φ_2 are the largest angles in the coordination sphere ($\tau = 0$ perfect square pyramid, $\tau = 1$ perfect trigonal bipyramid) we calculate $\tau = (170.8 - 164.4)/60 = 0.106$ for Mn(2), indicating a small trigonal distortion. The salicylato oxygen [O(7)] occupies the Jahn−Teller distorted apical position (Figure 1). The elongation is shown by a comparison of Mn(2)−N(1) = 1.982(2) Å and Mn(2)−O(4) = 1.950(2) Å the longest distances on the equatorial plane with the axial distance Mn(2)−O(7) = 2.142(2) Å. The Hsaladhp ligand acts as a tridentate chelating agent by using an imine nitrogen, and phenolate and alkoxide oxygen atoms to coordinate to Mn^{III}. The equatorial preference of the Schiff-base ligand has been reported for other mono-, di-, and trinuclear manganese complexes with this and related ligands.[11−20] The Mn^{III}−alkoxide oxygen distance [Mn(2)−O(2) = 1.876(2) Å] is equivalent to the Mn^{III}−phenolate oxygen distance [Mn(2)−O(1) = 1.862(2) Å] even though the former bridges to the Mn^{II} ion. The Mn(III)−alkoxide oxygen distance is also very similar to Mn^{IV}−alkoxide oxygen bonds reported for $Mn^{IV}(saladhp)_2$, $Mn-O_{av} = 1.889$ Å[11,12] and $[Mn^{IV}(hib)_3]^{2-}$, $Mn-O_{av} = 1.841$ Å.[31] The central ion Mn(1) and the terminal ions Mn(2) are bridged by alkoxide oxygens from the saladhp ligand, and two carboxylato oxygens from the salicylato ligands, resulting in a 3.495 Å Mn(1)···Mn(2) separation with a 119.98(8)° Mn(1)−O(alkoxide)−Mn(2) angle. The Mn(III) ions are displaced slightly out of the best least-squares plane defined by O(1), N(1), O(2), and O(4) toward the apical salicylate moiety, by 0.20 Å.

The cluster is valence trapped as evidenced by the long central Mn^{II} to heteroatom bond lengths and by Jahn−Teller distortion of the terminal high-spin Mn^{III} ions. The present compounds allow the certain assignment of the oxidation state for Mn(1) as a Mn^{II} and for Mn(2) as Mn^{III} ions, whereas in the trinuclear compounds $Mn^{III}Mn^{II}Mn^{III}(X\text{-}Hsaladhp)_2(AcO)_4(CH_3OH \text{ or } H_2O)_2$ for which the sixth position on the terminal manganese atom is occupied by a methanol or water molecule, the question could arise for a deprotonated rather than a protonated form of the ligand.

Magnetic Properties of 1. The molar magnetic susceptibility of **1** was measured as a function of temperature. The results are shown in Figure 2 in the form of μ_{eff}/3Mn vs *T*. The value of μ_{eff} decreases from 7.93 μ_B at 300 K to 3.15 μ_B at 3.2 K. The μ_{eff}/3Mn at room temperature, which is comparable to values previously reported[17,32] for $Mn^{III}Mn^{II}Mn^{III}(L)_2(\mu\text{-}AcO)_4(ROH)$ (L = tridentate ligand, R = H, CH_3) shows that there is a small antiferromagnetic interaction between the manganese atoms (spin-only value of 2 Mn^{III} and a Mn^{II} is 9.1 μ_B).

By virtue of crystallographic criteria the isotropic Heisenberg Hamiltonian for complex **1** is given by the eq 1,

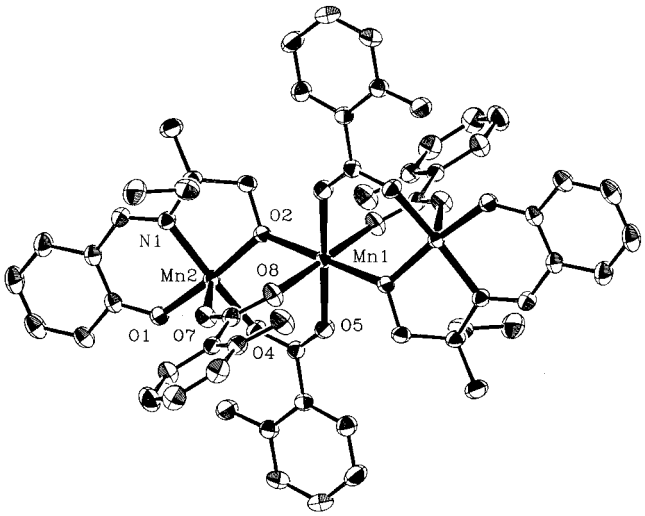

Figure 1. ORTEP view of complex **1** with 50% thermal ellipsoids showing the atom-labeling scheme around the Mn atoms.

Table 3. Selected Bond Distances(Å) and Angles (°) of **1**

Bond Distances (Å)			
Mn(1)···Mn(2)	3.495	Mn(2)−O(2)	1.876(2)
Mn(1)−O(2)	2.157(2)	Mn(2)−N(1)	1.982(2)
Mn(1)−O(5)	2.199(2)	Mn(2)−O(7)	2.142(2)
Mn(2)−O(1)	1.862(2)	Mn(2)−O(4)	1.950(2)
Values of Angles (°)			
O(8)−Mn(1)−O(2)	90.69(7)	O(2)−Mn(2)−N(1)	83.83(7)
O(8)−Mn(1)−O(5)	87.32(7)	O(4)−Mn(2)−N(1)	164.38(7)
O(2)−Mn(1)−O(5)	89.13(7)	O(1)−Mn(2)−O(7)	92.40(7)
O(1)−Mn(2)−O(2)	170.76(7)	O(2)−Mn(2)−O(7)	96.33(7)
O(1)−Mn(2)−O(4)	85.91(7)	O(4)−Mn(2)−O(7)	90.65(7)
O(2)−Mn(2)−O(4)	96.97(7)	N(1)−Mn(2)−O(7)	104.80(8)
O(1)−Mn(2)−N(1)	91.04(7)	Mn(2)−O(2)−Mn(1)	119.98(8)

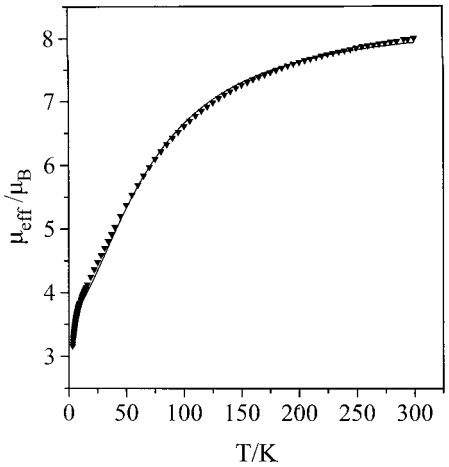

Figure 2. Magnetic susceptibility of **1** plotted as μ_{eff}/3Mn versus *T* with the fit to eq 5 (solid line).

(31) Saadeh, S. M.; Lah, M. S.; Pecoraro, V. L. *Inorg. Chem.* **1991**, *30*, 9.

(32) Baldwin, M. J.; Kampf, J. W.; Kirk, M. L.; Pecoraro, V. L. *Inorg. Chem.* **1995**, *34*, 5255.

$$H = -2J_1(S_1 \cdot S_2 + S_2 \cdot S_3) - 2J_2(S_1 \cdot S_3) \quad (1)$$

(**1** having an arrangement $S_1 - S_2 - S_3$) where $S_1 = S_3 = 2$ and $S_2 = {}^5/_2$. Because of the large distance between the terminal Mn^{III} ions (6.990 Å), we can exclude this interaction; therefore, the major exchange interaction is expected between the terminal Mn^{III} and the central Mn^{II}. This assumption is also based on an extended study for similar trinuclear complexes[17,20] where it has been proved that the role of the J_2 was unimportant in the fitting procedure. The exchange energies may be calculated by Kambe's method and are given by

$$E(S,S_{13}) = -J_1[S_T(S_T + 1) - S_{13}(S_{13} + 1) - S_2(S_2 + 1)] \quad (2)$$

For similar compounds, different g values have been assumed[17] for Mn^{III} and Mn^{II} in the Zeeman Hamiltonian and have added first- and second-order contributions to the Van Vleck equation. However the use of isotropic g values in the Zeeman term, dealing with the problem of mixed-valence polynuclear systems, also gives satisfactory magnetic models.[18] Assuming isotropic g values the Zeeman term was added to the preceding Hamiltonian

$$H_{ZEEMAN} = g\mu_B(S_1 + S_2 + S_3) \cdot B \quad (3)$$

A mean field correction zJ accounting for the weak interaction between trimers was added. As it has been stated[20] the role of the mean field correction in the low-temperature susceptibility data is quite important. The final expression of the susceptibility is given by

$$\chi_{MFC} = \frac{\chi_M}{1 - \dfrac{2zJ\chi_M}{N\mu_B{}^2 g^2}} \quad (4)$$

where χ_M is

$$\chi_M = (Ng^2\mu_B{}^2/3\kappa T)\frac{[\sum_i S_i(S_i + 1)(2S_i + 1)\exp(-E_i/\kappa T)]}{[\sum_i (2S_i + 1)\exp(-E_i/\kappa T)]} \quad (5)$$

The magnetic parameters obtained from the fitting procedure are $J_1 = -5.7$ cm^{-1}, $g = 2.02$, $zJ = -0.19$ cm^{-1}, $R = 0.004$ where

$$R = \sum_n [(\mu_{eff})_{exptl} - (\mu_{eff})_{calc}]^2 \quad (6)$$

Energy levels are represented in Figure 3 with the addition of S_{13} label. The ground state is found to be the

$$|S_2 = {}^5/_2, S_{13} = 4, S = {}^3/_2\rangle \quad (7)$$

The energy scheme obtained from the susceptibility data is further verified by the isothermal magnetization measurements at 4 K and up to 5 T. The data are given in Figure 4. The two solid lines represent the theoretical magnetization behavior of $S = {}^3/_2$, $S = {}^1/_2$ states and are calculated from the expression

$$M = Ng\mu_B SB_s(\chi) \quad (8)$$

where $B_s(\chi)$ is the Brillouin function for states with $S = {}^3/_2$ and $S = {}^1/_2$. This clearly shows that the lowest lying state was the $S = {}^3/_2$ with reasonable population of a state, or states, of lower spin.[17] Usually from the magnetization curve we can obtain the

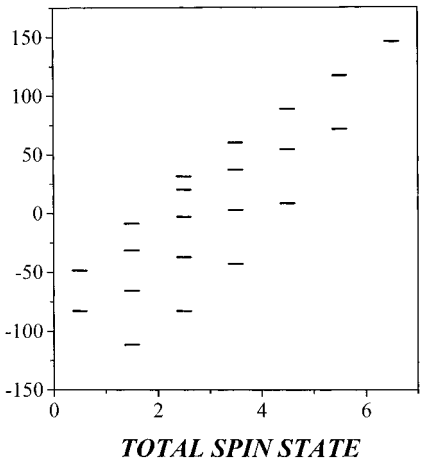

Figure 3. Spin levels for **1**. The energy in cm^{-1} is given as a function of the spin value.

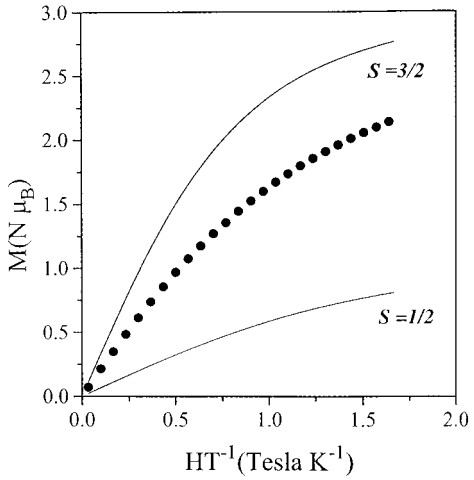

Figure 4. Magnetization study for **1** at 4 K over the field range 0−2 *T* as a function of H/T. The solid lines represent the theoretical curves for $S = {}^3/_2$ and $S = {}^1/_2$ states.

D value easily if it is assumed that the ground state is isolated.[8] In the present study we have the population of the first excited state along with the ground state. So the depopulation of the states does not follow the Boltzmann distribution that means we cannot use an appropriate formula to calculate the effect of the zero field splitting in the depopulation of the states.

EPR Study of 1. The EPR spectrum shown in Figure 5 is obtained at 4 K when **1** is dissolved in $CHCl_3$. The low-field EPR signal is a superposition of two signals, one centered around $g = 3.6$ and the other, where hyperfine structure is observed, centered around $g = 4.1$ indicating a $S = {}^3/_2$ state and a multiline signal at $g = 2$ with ~19 lines. The hyperfine structure in the $g = 4.1$ signal is consistent with previous reports[14,20] and shows characteristics similar to those of the manganese cluster in the S_2 state of the OEC.[3,4] The other signal at $g = 3.6$ propably comes from excited state(s). Therefore, the simple observation of multiline or $g = 4.1$ signals in a model compound may provide little structural insight for the manganese in the OEC. The observed EPR spectrum is assigned to the trinuclear compound **1**, because there is no dissociation of this complex in $CHCl_3$. The EPR spectra in MeOH show a classic six-line signal centered at $g = 2$ from uncomplexed Mn^{II} due to dissociation of the complexes to form monomeric units of $[Mn^{II}(Hsal)_4]^{2-}$ and $[Mn^{III}(Hsaladhp)]^+$ as shown by ^{1}H NMR

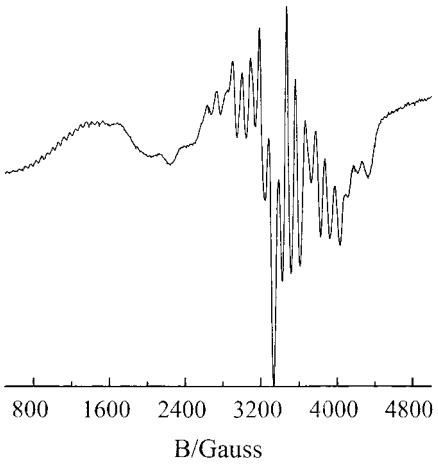

Figure 5. X-band EPR spectra of **1** in $CHCl_3$ glassy solution at 4 K in the range 400−4800 G.

study.[33] The conductance of MeOH solution indicates that a 2:1 electrolyte is formed.

Simulation Properties. To verify the previous assignment a simulation procedure was carried out based on the following Hamiltonian formalism,[34]

$$H = \mu_B BgS + SAI \tag{9}$$

with the following assumptions: (a) The electronic Zeeman interaction is the largest, followed by the hyperfine interaction: (b) To increase the accuracy of the simulation a second-order perturbation theory carried outcomes[35]; (c) The only populated state is the ground state, $S = {}^3/_2$, and is well "isolated" from the next nearest excited states; (d) The line widths (W) can vary as a function of the direction of the externally applied magnetic field,[34,35]

$$W(l_x,l_y,l_z) = \sqrt{w_x^2 l_x^2 + w_x^2 l_y^2 + w_z^2 l_z^2} \tag{10}$$

where the l_x, l_y, l_z are the direction cosines of the magnetic field on the electronic Zeeman principal axes and w_x, w_y, and w_z are the line widths along the principal axes; (e) isotropic values for hyperfine interactions (different values for Mn(II) and Mn(III)) and g values [the same for Mn(II) and Mn(III)]. To avoid overparametrization of the simulation model we used hyperfine values close to the one observed in the literature for Mn(II) and Mn(III), a small line widths anisotropy, and a mixture of Lorentzian−Gaussian shape in 0.75/0.25 ratio.

The multiline spectra at $g = 2$ in Figure 5 is simulated and the following parameters obtained from the simulation procedure of the trinuclear system Mn(III)Mn(II)Mn(III) (I_1, I_2, $I_3 = {}^5/_2$, $S = {}^3/_2$): $A = 140$ (10^{-4} cm^{-1}) for Mn(III), $A = 90$ (10^{-4} cm^{-1}) for Mn(II); w_x, $w_y = 75$ G, $w_z = 50$ G; $g = 1.99$. These values, in line with previous reports, emphasize the trinuclear nature of the multiline spectra while the results are shown in Figure 6. Using the A values for Mn(II) and Mn(III) obtained from the previous simulation, a new simulation was performed for the case of a hypothetical dimer, instead of trimer, Mn(III)−Mn(II), and the resulting spectrum is shown in Figure 6. The difference between the two simulated spectra reveals the trinuclear character of the X-band EPR spectra.

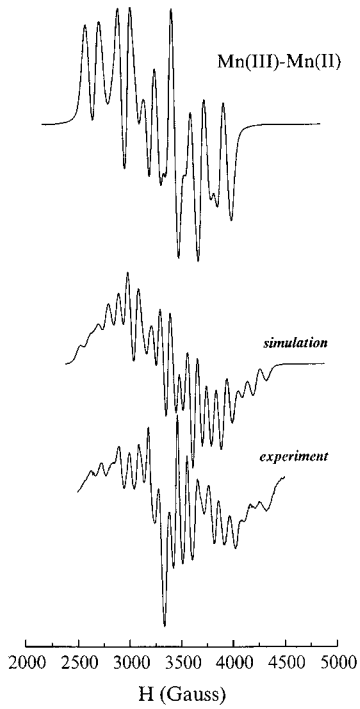

Figure 6. A simulation (top drawing) of a hypothetical Mn(III)−Mn(II) dimer, using the A values for Mn(II) and Mn(III) obtained from the simulation below. Simulated and experimental EPR spectra following parameters obtained from the simulation procedure of the trinuclear system Mn(III)Mn(II)Mn(III) ($I_1 = I_2 = I_3 = {}^5/_2$, $S = {}^3/_2$): $A = 140$ (10^{-4} cm^{-1}) for Mn(III); $A = 90$ (10^{-4} cm^{-1}) for Mn(II); w_x, $w_y = 75$ G, $w_z = 50$ G; $g = 1.99$.

Table 4. ^{1}H NMR Data and Signal Assignment of the Mn(III)/Mn(II)/Mn(III) Trimer Complex in $CDCl_3$ Measured at 500 MHz (T = 296 K)[a] (Chemical Shift Values Are Also Measured in $CDCl_3$/THF 90:10 v/v Mixture.)

peak	assignment	intensity	$CDCl_3$ (ppm)	T_1 (ms)	$CDCl_3$/THF-d_8 9:1 (ppm)
A	Hsaladhp **CH=N**	2	210[a]	*b*	−
1	Hsaladhp **CH_2**	1	37.2	0.5	*c*
1′	Hsaladhp **CH_2OH**	4	5.0−2.0	*d*	−
B	Hsal **5,5′**	(2 + 2)	22.4	0.8	24.9
C	Hsal **5,5′**		19.9	0.8	23.8
5,5′	Hsaladhp	(1 + 1)	12.7	3.6	12.7
5,5′	Hsaladhp		10.4	3.1	10.8
2	Hsaladhp **CH_3**	(6)	11.3	3.5	11.8
3,3′	Hsaladhp	(1 + 1)	6.6	1.9	−
3,3′	Hsaladhp	(1 + 1)	4.0	1.9	−
S	Hsal **4,4′, 3,3′, 2,2′**	(2 + 2 + 2)	5.0−2.0	*d*	−
S′	Hsal **4,4′, 3,3′, 2,2′**	(2 + 2 + 2)	5.0−2.0	*d*	−
4,4′	Hsaladhp	(1 + 1)	−17.7	4.7	−19.9
4,4′	Hsaladhp		−18.9	4.7	*c*
6,6′	Hsaladhp	(1 + 1)	−26.3	3.9	−26.6
6,6′	Hsaladhp		−26.7	3.9	*c*

[a] Measured at 200 MHz. [b] Not measured; probably shorter than 0.1 ms. [c] Not observed. [d] Not measured because of the presence of many signals in the region from 6.00 to 0.00 ppm.

^{1}H NMR Study. Because no similar examples of mixed-

(33) Pecoraro, V. L. In *Manganese Redox Enzymes;* VCH Publishers Inc.: New York, 1992; p 207.
(34) Abragam, A.; Bleaney, B. *Electron Paramagnetic Resonance of Transition Ions*; Clarendon Press: Oxford, 1970.
(35) Pilbrow, J. R. *Transition Ion Electron Paramagnetic Resonance*; Clarendon Press: Oxford, 1990.

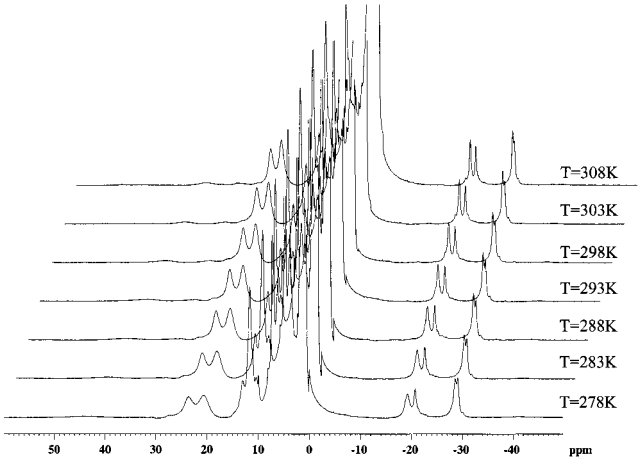

Figure 7. Variable temperature 500 MHz ^{1}H NMR spectra of manganese(III/II/III) trinuclear compound in $CDCl_3$.

Table 5. Temperature Dependence of Hyperfine Shifted Signals of Mn(III)/Mn(II)/Mn(III) Trimer Complex Measured at 500 MHz

peak	278	283	288	293	298	303	308
1	43.36	42.14	40.53	38.85	37.21	36.14	34.60
B	23.45	23.25	22.91	22.64	22.40	22.20	21.96
C	20.59	20.35	20.18	20.03	19.93	19.91	19.86
5	12.98	12.95	12.90	12.81	12.71	12.61	12.51
2	11.61	11.51	11.44	11.39	11.34	11.24	11.17
4	−19.24	−18.73	−18.36	−18.00	−17.66	−17.36	−17.05
4′	−20.71	−20.24	−19.76	−19.34	−18.93	−18.51	−18.14
6	−28.64	−27.97	−27.40	−26.83	−26.30	−25.83	−25.34
6′	−29.10	−28.47	−27.83	−27.27	−26.71	−26.20	−25.69

valence Manganese-trimer compounds exist in the bibliography, the assignment of the proton resonances is tentative. Acquired NMR data are discussed and analyzed in terms of relaxation times, paramagnetic shift, and signal intensity, but compared with data reported for nickel(II) salicylideneamino-like complexes.[36] Proton assignment and longitudinal relaxation times are reported at Table 4. Spectra recorded in the temperature

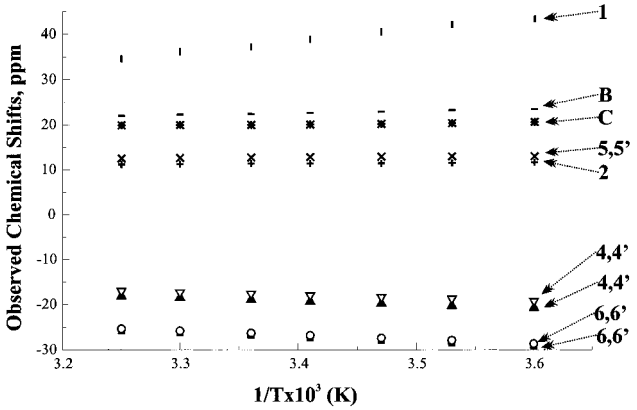

Figure 8. Curie plots of hyperfine shifted signals of manganese(III/II/III) trinuclear compound.

range 278−308 K are illustrated at Figure 7 and the temperature dependence of chemical shifts for hyperfine shifted signals is presented at Figure 8. Measured chemical shift values for the temperature range 278−308 K are reported in Table 5. All signals show a Curie-type temperature dependence. In the Ni(II) complex, protons are found to be shifted dramatically. Signals are spread in a range of about 500 ppm as an effect of spin delocalization which may occur through the oxygen atom and the −C═NR group. In the Ni(II) complex the proton resonances of the aromatic ring were observed as four sets of double-hyperfine shifted resonances, whereas the proton resonances of the −CH═N group are found to be the most paramagnetically shifted signals (up to 420−480 ppm).

According to this, the broad signal at 210 ppm (observed in the spectra recorded at 200 MHz) is attributed to the −CH═N proton and the broad signal at 37.2 ppm, **A**, is attributed to the $-CH_2-O-$ group of the salicylideneamino group. The assignment of those protons is supported further by their T_1 values, because −CH═N and **A** protons are the protons closer to the

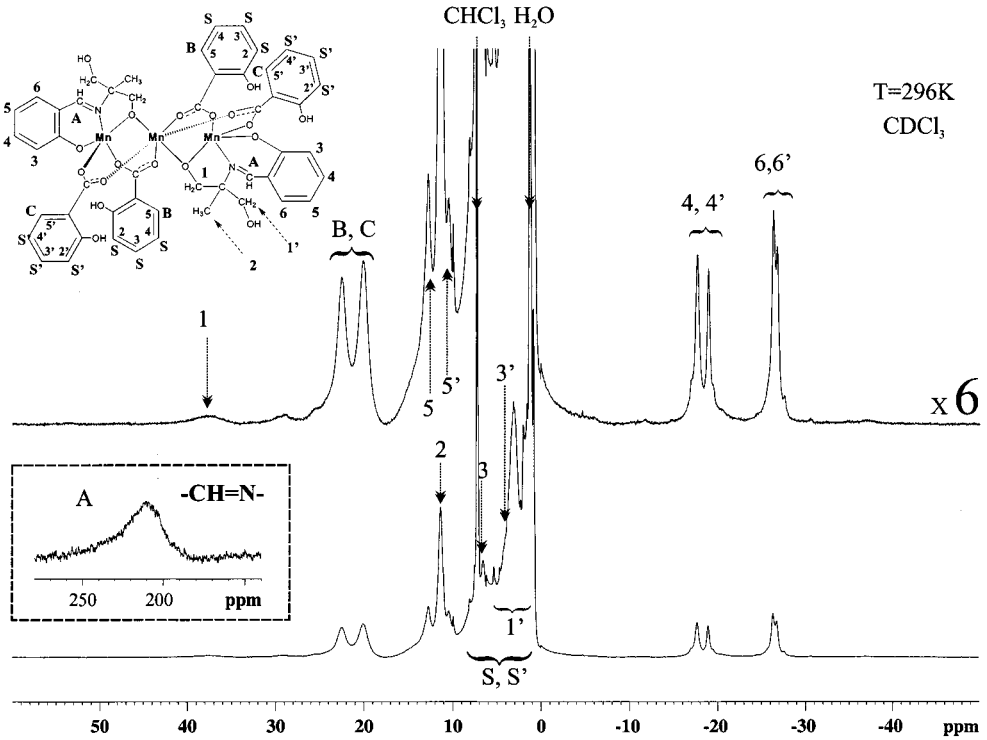

Figure 9. 500 MHz 296 K ^{1}H NMR spectra of manganese(III/II/III) trinuclear compound in deuterated chloroform.

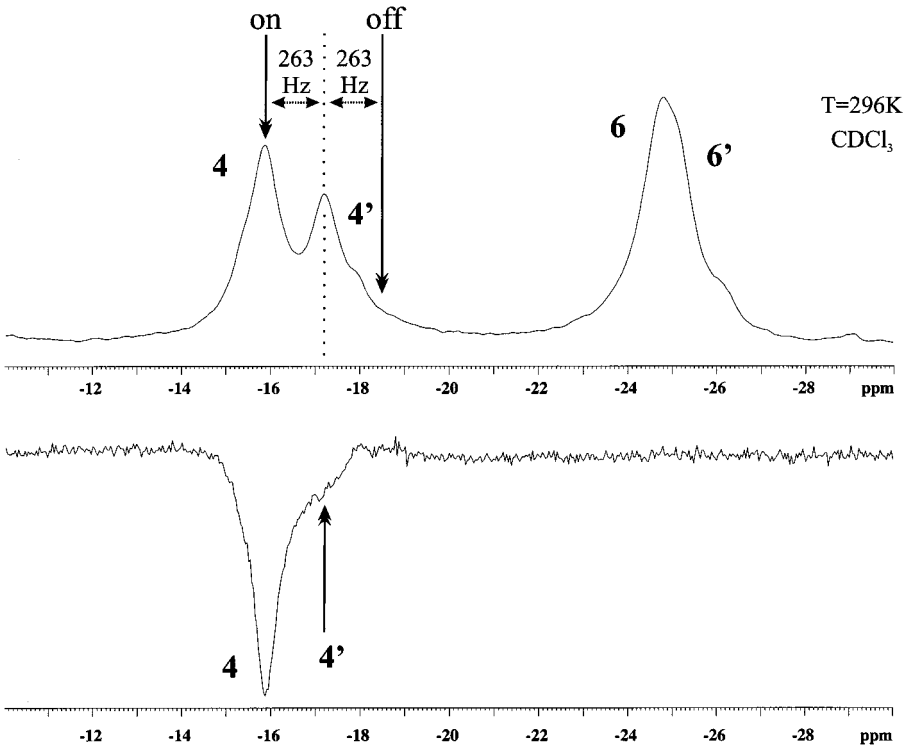

Figure 10. 200 MHz 296 K ^{1}H NMR spectra of manganese(III/II/III) trinuclear compound in $CDCl_3$. The upper trace represents the reference spectrum. The other traces are 1D NOE difference spectra. The traces are labeled according to saturated signals. The 1D difference spectra are obtained with the on−off (right) acquisition scheme described elsewhere.[24,25]

metal center (C7 and C9 in the crystal structure). Additionally, **A** is the most shifted signal from the diamagnetic spectral region (excluding −CH═N) and has the shortest relaxation time among the paramagnetically shifted signals (see Table 4).

Spin delocalization mechanisms similar to those that occur in the Ni(II) complex should be anticipated for the manganese trimer. However, the expected sign of net spin density on the ligand for a metal-to-ligand saladhp spin-transfer mechanism in Mn(III) and Mn(II) (d^4 and d^5, respectively) is expected to be opposite that[37] of Ni(II) (d^8). In this trinuclear Mn complex where the three metals are magnetically coupled, the central metal, Mn(II) $S = {}^5/_2$, present spins antiparallel to the magnetic field and the sign of spin density delocalized on ligands is expected to be opposite to that of a Mn(III), that is the same as in Ni(II). However, the presence of the two Mn(III) ions with $S = 2$ [$S = {}^3/_2$ for the trinuclear Mn(III)/Mn(II)/Mn(III) complex] accounts for a total sign of net spin density the reverse of that for the Ni(II) complex and protons strongly influenced by the paramagnetism of the metalic core are expected to be shifted upfield.

Consequently, the two sets of double peaks are observed at about −18 and −26 ppm (Figure 9), signals **4**, **4′** and **6**, **6′** could be assigned to the aromatic protons of Hsaladhp ligand. The fact that four set of double peaks are also observed for the 8 (2 × 4) protons of the two aromatic rings in Ni(II) complex is rationalized by the inequivalence of the two aryl groups due to two possible conformers in solution.[36,38]

Chemical exchange should also been taken into account. 1D difference spectra at 200 MHz (Figure 10), show that by saturating signal **4** strong negative effect (saturation transfer) with signal **4′** is observed. Because the molecule is expected to be in the fast motion limit, negative NOEs in 1D difference spectra can only be due to chemical exchange.[38] The same experiment is performed for signals **6**, **6′** but since the two signals are close, selective saturation of only one of the signals is extremely difficult.

Chart 1. Molecular Formula of Mixed-Valence Manganese(III/II/III) Trimer

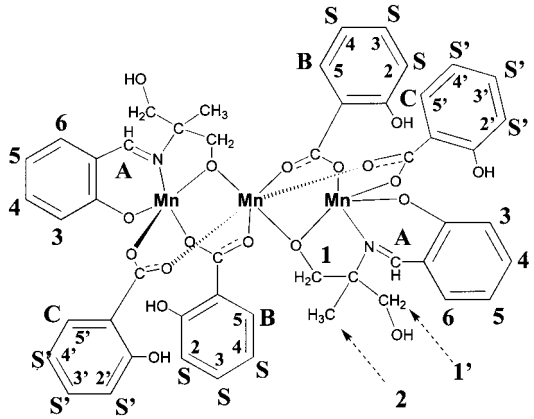

Thus, those signals are attributed to the 4 and 6 aromatic protons of the saladhp ligand, respectively (see also Chart 1) by analogy to the same signals of Ni complex which are the most shifted aromatic proton signals.[36,38] Additionally, the two proton resonances at −18 ppm, **4**, **4′**, present identical T_1 values, and the same is also observed for the two resonances appearing at −26 ppm (signals **6**, **6′**).

The possibility of an existed equilibrium between two different conformations of salicylideneamino groups in solution, is supported further by spectral data aquired in mixture $CDCl_3$/THF-d_8 9:1, v/v (Figure 11). Each of the two pair of peaks (**4**, **4′** and **6**, **6′**) was replaced by one signal, whereas signal **A** was not observed. The intensity of each one of the upfield signals (at −19.8 and −26.6 ppm) in 10% THF corresponds to two protons. These findings could point out to minor or major conformational changes in the presence of THF. Possible

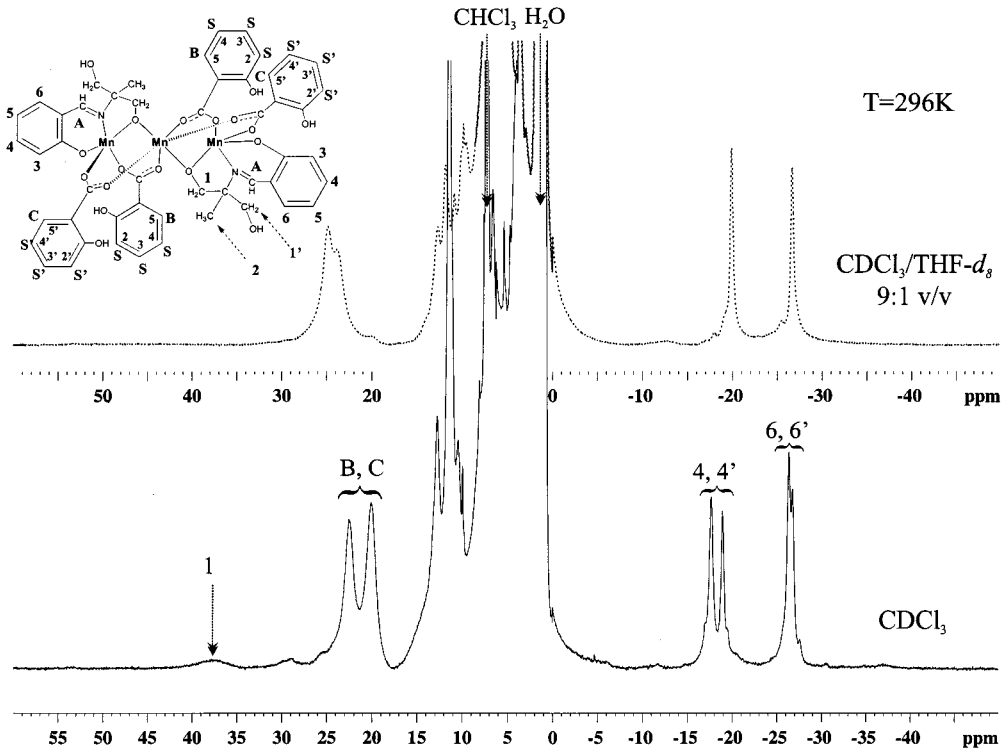

Figure 11. 500 MHz 296 K ^{1}H NMR spectra of manganese(III/II/III) trinuclear compound in $CDCl_3$ (lower trace) and in $CDCl_3$/THF-d_8 9:1 v/v (upper trace).

coordination of THF to the metal probably accounts for intramolecular structural rearrangements in solution manifested by the degeneration of the Hsaladhp aromatic proton signals. The two conformers seem to be in 1:1 ratio in $CDCl_3$ and observed changes in signal intensities could be discussed in terms of different ratio of the two forms (approximately 9:1 considering the 1D spectra at $CDCl_3$/THF-d_8 9:1) or in terms of fast exchange between the two conformers even if the ratio between them remains 1:1. This is also evident in spectra acquired in different temperatures where the intensity of **4**, **4′** and **6**, **6′** signals is changing upon the temperature changes (see also Figure 7).

The chemical shifts of the other two sets of protons (denoted as **3**, **3′** and **5**, **5′)**, corresponding to the 3 and 5 protons, respectively, seem to be only slightly influenced by the paramagnetism of the metal, compared with the 4 and 6 protons, and thus are moderately shifted and found closer to the diamagnetic region. Consequently, the resonances observed at 6.6, 4.0 ppm and 12.7, 10.4 ppm, are attributed to 3 and 5 protons, respectively. **3**, **3′** signals exhibit identical longitudinal relaxation times (as observed for the other aromatic protons), whereas in signals **5**, **5′** the measured T_1 values are very similar. Finally, the signal at 11.8 ppm is attributed to the $-CH_3$ group (signal denoted as **2)** of the Hsaladhp ligand, according to its intensity. The intensity ratio between signal **2** and **4**, **4′** or **6**, **6′** is 3:1 (considering two equivalent methyl groups of salicylideneamino group). Thus, the only unassigned protons, denoted as **1′**, belonging to the saladhp ligand are those of crystallographic C10. Those protons are two-bond far away from the nitrogen of the Hsaladhp ligand and far from the metal center; thus they are expected not to be dramatically shifted out from the diamagnetic region. Protons in β-position with respect to the nitrogen are found at the region between 0 and 5 ppm in the case of nickel bis(salicylideneamino)-type complex and this seems to be the case for the Mn trimer, as well. The only paramagnetically shifted signals remained unassigned are the broad signals denoted as **B** and **C** at the region 20−22 ppm. The intensity of each peak is twice the intensity measured for each upfield shifted signal of Hsaladhp (signals **4**, **4′**, **6**, **6′**). Taking into account that there are four salicylato ligands, each signal corresponds to a pair of equivalent aromatic protons and the closest proton of salicylato group to the metal should be that at positions 5, 5′. The two signals, **B** and **C**, present identical relaxation times, and therefore are assigned to those protons. Since no other signal of similar intensity is observed out of the diamagnetic region the resonances of the other aromatic protons should lie in the region 5−2 ppm. A detailed assignment of those resonances was not attempted.

Conclusion

Although mixed-valence and homovalence trimers have been reported previously, very interesting features are presented in this report. Compound **1** is the first example of structurally characterized, mixed-valence, open-structure trimers that was not on the sixth position of the terminal manganese atoms a ligand, a fact which allows a certain assignment of the oxidation state of it as Mn^{III}. The $g = 2$ multiline signal of the S_2 oxidation state of the water-oxidation manganese center has provided the basis for much speculation as to the nuclearity and oxidation states of the manganese ions in the OEC. Mixed-valence dimers, such as Mn(III/II) or Mn(III/IV) and tetranuclear Mn(III/III/III/IV) compounds,[5e,8] exhibit multiline features. A recent theoretical approach[39] tends to the conclusion that a tetranuclear cluster is responsible for the EPR signal and that the hyperfine

(36) Bertini, I.; Luchinat, C. In *NMR of Paramagnetic Molecules in Biological Systems;* Benjamin/Cummings: Menlo Park, CA, 1986.
(37) La Mar, G. N. *NMR of Paramagnetic Molecules;* La Mar, G. N., Horrocks W. DeW, Jr., Holm, R. H., Eds.; Academic Press: New York, 1973; pp 86−126.
(38) Bertini, I.; Luchinat, C. *Coord. Chem. Rev.* **1996**, 150.
(39) Zheng, M.; Dismukes, G. C. *Inorg. Chem*. **1996**, *35*, 3307.

couplings must be anisotropic.[40] This study[39] also suggests that the Mn(III) ion(s) may be five-coordinate, having a distorted-trigonal bipyramidal geometry with an $(e')^2(e'')^2$ configuration. A possible explanation given as to why there could be five-coordinate Mn(III) ions in the S_2 state of the OEC is that one or both of the substrate water molecules may not be bound (yet) to manganese cluster. Therefore, the presence of five-coordinate Mn atoms in 1, which is unique among trinuclear complexes, could provide an interesting case for studying the effects the coordination of water on the spectroscopic and structural features of such clusters. Also, among the known Mn clusters, the compound reported here exhibits the unique feature of possessing a 19-line EPR signal similar to that of the OEC (Figure 12). Although EPR spectroscopy cannot be used as a structural tool to resolve complicated problems of this type, it is nevertheless interesting that the multiline signal of OEC has not been reproduced by any Mn complex so far. Unfortunately a $[Mn_4]$ model satisfying the number of lines, the line shapes and widths and anisotropic hyperfine coupling and five-coordinate Mn(III) ion has not yet been reported. It is remarkable that the structure presented in this report, although not a tetranuclear complex, satisfies all the above characteristics, and thus could be considered relevant to the trimer/monomer model [3Mn + 1Mn] which is one of those proposed for the OEC.[1a,41,42]

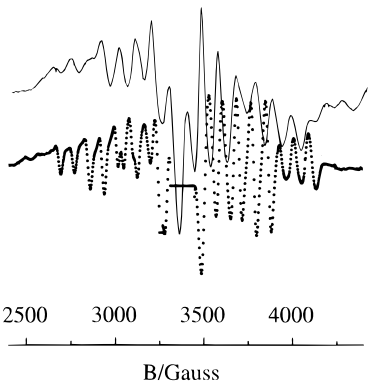

Figure 12. A superposition of the two multiline EPR signals of complex 1 (—) and of PSII (●) measured under the following experimental conditions: Light minus dark difference spectra of PSII-enriched membranes illuminated at 200 K for 4 min. EPR conditions: 9.4125 GHz, T = 11 K, modulation ampl. 25 Gpp, microwave power 31 mW.

Acknowledgment. The authors wish to thank Prof. Ivano Bertini and Prof. Claudio Luchinat for his assistance in the interpretation of the ^{1}H NMR data and the Large Facility Scale Laboratory in Florence for collecting the NMR data. EPR spectra of the S_2 state of PSII were kindly provided by Dr. C. Goussias.

Supporting Information Available: Tables giving magnetic susceptibility data in the temperature range 3−300 K and a CIF file. This material is available free of charge via the Internet at http://pubs.acs.org.

IC991430X

(40) Kim, D. H.; Britt, R. D.; Klein, M. P.; Sauer, K. *Biochemistry* **1992**, *31*, 541.
(41) Pecoraro, V. L.; Kessissoglou, D. P.; Li, X−h.; Lah, M. S.; Saadeh, S.; Bender, C. A.; Bonadies, J. A.; Larson, E. *Curr. Res. Photosynth.* **1990**, *I*, 709.
(42) Debus, R. J. *Biochim. Biophys. Acta* **1992**, *1102*, 269.